ResearchGate

See discussions, stats, and author profiles for this publication at: https://www.researchgate.net/publication/281389826

Development of a new corona discharge based ion source for high resolution time-of-flight chemical ionization mass spectrometer to measure gaseous H2SO4 and aerosol sulfate

ARTICLE *in* ATMOSPHERIC ENVIRONMENT · OCTOBER 2015

Impact Factor: 3.28 · DOI: 10.1016/j.atmosenv.2015.08.028

READS

24

7 AUTHORS, INCLUDING:

Jun Zheng

Nanjing University of Information Science …

10 PUBLICATIONS **221** CITATIONS

SEE PROFILE

All in-text references underlined in blue are linked to publications on ResearchGate, letting you access and read them immediately.

Available from: Jun Zheng
Retrieved on: 24 January 2016

Atmospheric Environment 119 (2015) 167–173

Contents lists available at ScienceDirect

Atmospheric Environment

journal homepage: www.elsevier.com/locate/atmosenv

Technical note

Development of a new corona discharge based ion source for high resolution time-of-flight chemical ionization mass spectrometer to measure gaseous H_2SO_4 and aerosol sulfate

Jun Zheng [a, b, *], Dongsen Yang [a, b], Yan Ma [a, b], Mindong Chen [a, b], Jin Cheng [a, b], Shizheng Li [a, b], Ming Wang [a, b]

[a] Collaborative Innovation Center of Atmospheric Environment and Equipment Technology, Nanjing University of Information Science & Technology, Nanjing 210044, China
[b] Yale-NUIST Center on Atmospheric Environment, Nanjing University of Information Science & Technology, Nanjing 210044, China

HIGHLIGHTS

- A new corona discharge ion source was developed for the Aerodyne HRToF-CIMS.
- The CD ion source was non-radioactive and non-corrosive.
- Both gaseous H_2SO_4 and aerosol sulfate can be detected by the CD-HRToF-CIMS.

ARTICLE INFO

Article history:
Received 27 March 2015
Received in revised form
8 July 2015
Accepted 11 August 2015
Available online 14 August 2015

Keywords:
Sulfuric acid
Sulfate
Corona discharge
HRToF-CIMS
Hydroxyl radicals

ABSTRACT

A new corona discharge (CD) based ion source was developed for a commercial high-resolution time-of-flight chemical ionization mass spectrometer (HRToF-CIMS) (Aerodyne Research Inc.) to measure both gaseous sulfuric acid (H_2SO_4) and aerosol sulfate after thermal desorption. Nitrate core ions (NO_3^-) were used as reagent ions and were generated by a negative discharge in zero air followed by addition of excess nitrogen dioxide (NO_2) to convert primary ions and hydroxyl radicals (OH) into NO_3^- ions and nitric acid (HNO_3). The CD-HRToF-CIMS showed no detectable interference from hundreds parts per billion by volume (ppbv) of sulfur dioxide (SO_2). Unlike the atmospheric pressure ionization (API) ToF-CIMS, the CD ion source was integrated onto the ion–molecule reaction (IMR) chamber and which made it possible to measure aerosol sulfate by coupling to a filter inlet for gases and aerosols (FIGAERO). Moreover, compared with a quadrupole-based mass spectrometer, the desired HSO_4^- signal was detected by its exact mass of m/z 96.960, which was well resolved from the potential interferences of $HCO_3^-\cdot(H_2O)_2$ (m/z 97.014) and $O^-\cdot H_2O\cdot HNO_3$ (m/z 97.002). In this work, using laboratory-generated standards the CD-HRToF-CIMS was demonstrated to be able to detect as low as 3.1×10^5 molecules cm^{-3} gaseous H_2SO_4 and 0.5 μg m^{-3} ammonium sulfate based on 10-s integration time and two times of the baseline noise. The CD ion source had the advantages of low cost and a simple but robust structure. Since the system was non-radioactive and did not require corrosive HNO_3 gas, it can be readily field deployed. The CD-HRToF-CIMS can be a powerful tool for both field and laboratory studies of aerosol formation mechanism and the chemical processes that were critical to understand the evolution of aerosols in the atmosphere.

© 2015 Elsevier Ltd. All rights reserved.

1. Introduction

Gas-phase sulfuric acid (H_2SO_4) is one of the most critical parameters to fully understand the mechanisms governing the new particle formation process and thus the total aerosol number concentration in the atmosphere (Kulmala et al., 2013, 2014; Sipila

* Corresponding author. School of Environmental Science and Engineering, Nanjing University of Information Science & Technology, Nanjing 210044, China.
E-mail address: zheng.jun@nuist.edu.cn (J. Zheng).

http://dx.doi.org/10.1016/j.atmosenv.2015.08.028
1352-2310/© 2015 Elsevier Ltd. All rights reserved.

et al., 2010; Zhang, 2010; Zhang et al., 2012). It is well established that H_2SO_4 is formed from sulfur dioxide (SO_2) through oxidation processes initiated by hydroxyl radicals (OH) (R1 to R3) (Finlayson-Pitts and Pitts, 1999; Seinfeld and Pandis, 1998).

$$SO_2 + OH + M \rightarrow HSO_3 \quad (R1)$$

$$HSO_3 + O_2 \rightarrow SO_3 + HO_2 \quad (R2)$$

$$SO_3 + H_2O \rightarrow H_2SO_4 \quad (R3)$$

Recent field and laboratory studies (Mauldin et al., 2012) have suggested that stabilized Criegee intermediates (SCIs) and their derivatives can contribute significantly to H_2SO_4 formation in the atmosphere. Regardless the origins, sulfate is often found to be one of the dominant aerosol components around the world (Jimenez et al., 2009) and thus can significantly affect aerosols ability to interact with solar/terrestrial radiations and to participate in cloud formation (IPCC, 2007).

Measurement of H_2SO_4 is difficult due to its low ambient concentration (typically much less than 10^7 molecules cm^{-3}) and being prone to wall losses. So far, chemical ionization mass spectrometry (CIMS) is the only available technique that is capable of detecting H_2SO_4 in the atmosphere (Berresheim et al., 2000; Eisele and Tanner, 1993; Kukui et al., 2008; Mauldin et al., 2003; Zheng et al., 2010, 2011). In general, nitrate core ions ($NO_3^-\cdot[HNO_3]_n$, where n = 0, 1, or 2) are the most widely used reagent ions for H_2SO_4 measurements (R4) because of their high selectivity with no humidity dependence (Viggiano et al., 1997).

$$H_2SO_4 + NO_3^-(HNO_3) \rightarrow HSO_4^- + (n+1)HNO_3 \quad (R4)$$

Typically, NO_3^- core ions are generated by a radioactive ion source, i.e., bombarding gaseous HNO_3 with α-particles (Am-241 or Po-210) followed by chemical ionization at atmospheric pressure, which is often referred as API-NO_3^--CIMS. Evidently, Ionization at atmospheric pressure has the advantages of higher chemical ionization efficiency and easier sample handling (Andrade et al., 2008) over the traditional negative ion CIMS (Huey, 2007). Therefore, the API-NO_3^--CIMS is capable of detecting less than 10^5 molecules cm^{-3} H_2SO_4 for 10-min integration time or less (Berresheim et al., 2000; Eisele and Tanner, 1993; Zheng et al., 2010). However, because of the ever-increasing safety concerns on radioactive materials, strict administrative regulations make shipping and field deploying CIMS instruments with a radioactive ion source difficult. Consequently, non-radioactive corona discharge (CD) ion sources have been developed for measurements of H_2SO_4 (Kurten et al., 2011) and HO_x free radicals (Kukui et al., 2008).

Corona discharge is essentially a type of electrical discharge formed between two electrodes when the air in-between is ionized by a potential of a few kilovolts or higher. The initial primary ions formed from a CD in air are dominated by O^- and O_2^- (R5 and R6),

$$O_2 + e^- \rightarrow O^- + O \quad (R5)$$

$$O_2 + e^- \rightarrow O_2^- \quad (R6)$$

which can further evolve into O_3^-, CO_3^-, CO_4^-, OH^-, HCO_3^-, NO_2^-, NO_3^- core ions, and their clusters (Nagato et al., 2006; Sekimoto and Takayama, 2007; Skalny et al., 2008) in the presence of trace amounts of water (H_2O) and carbon dioxide (CO_2). The detailed reaction mechanisms to form these primary ions are well studied and it is believed that NO_3^- core ions will become the dominant negative ions within a few milliseconds. In addition, substantial amounts of neutral species, such as ozone (O_3) and nitrogen oxides (NO_x = NO + NO_2) are also formed (Franzblau, 1991) (R7 to R11).

$$O + O_2 + M \rightarrow O_3 \quad (R7)$$

$$N_2 + e^- \rightarrow N^- + N \quad (R8)$$

$$N + O + M \rightarrow NO \quad (R9)$$

$$N + O_2 \leftrightarrow NO + O \quad (R10)$$

$$O_3 + NO \rightarrow NO_2 + O_2 \quad (R11)$$

Moreover, hydroxyl radical (OH) can also be generated (R12) and its production rate is believed to be enhanced by water concentration (Nagato et al., 2006). Some OH will react with NO_2 to produce HNO_3 (R13), however significant amounts of OH can remain intact and lead to H_2SO_4 production when SO_2 is present (R1 to R3).

$$O^- + H_2O \rightarrow OH^- + OH \quad (R12)$$

$$OH + NO_2 + M \rightarrow HNO_3 \quad (R13)$$

Therefore, a CD ion source may potentially interfere with H_2SO_4 measurement when used with an API-NO_3^--CIMS (Tanner et al., 1997). Using HNO_3 as reagent gas, Kurten et al. (2011) have demonstrated that a CD ion source can be used in an API-NO_3^--CIMS setup showing a small cross-sensitivity to 1 parts per million by volume (ppmv) SO_2, equivalent to ~3×10^4 molecules cm^{-3} H_2SO_4. To eliminate this potential interference completely, Kukui et al. (2008) have added a port at the outlet of the CD ion source to provide a small counter flow of pure air, preventing the neutral species from entering the ion–molecule reaction chamber. Although CD is relative safe to operate, HNO_3 is a highly corrosive chemical and excessive exposure to HNO_3 due to accidental release or long-term usage may cause damages to the spectrometer hardware. Incidences have been reported that use of HNO_3 has caused leakage of radioactive materials into the exhaust systems of several API-NO_3^--CIMS units. Therefore a non-radioactive and non-corrosive ion source is desirable for the safe operation of CIMS, especially for H_2SO_4 detection.

In this work, we developed a new CD ion source to couple with a commercial HRToF-CIMS (Aerodyne Research Inc.) (Zheng et al., 2015). NO_3^- ions were produced in two steps, using both zero air and NO_2 as the reagent gases. The performance of the CD-HRToF-CIMS was evaluated with laboratory-generated gaseous H_2SO_4 and particulate sulfate samples.

2. Experimental methods

2.1. CD ion source and ion chemistry

Fig. 1 is the schematic diagram of the CD ion source and the IMR portion of the HRToF-CIMS. The CD ion source mainly consisted of a 30-mm long stainless steel needle, one 6.4-mm tube OD Swagelok PFA tee and one 6.4-mm tube OD Swagelok stainless steel tee. They were inter-connected with two pieces of 25-mm long, 6.4-mm OD stainless steel tubing. The needle was insulated from the tube by Torr-Seal (Varian Vacuum Inc.) and the gap between the needle tip and the tube was about 1.5 mm. The CD was initiated by applying about −1700 V to the needle and the metal tube was grounded through a 1.0 MΩ resister. The CD current was maintained at ~ 1.6 mA to achieve a stable reagent ion concentration. About 0.62 standard liters per minute (SLPM) of zero air was fed into the CD to serve as both carrier gas and reagent gas. Immediately downstream of the CD tube, about 0.48 SLPM of 200 ppmv NO_2 (Nanjing Special

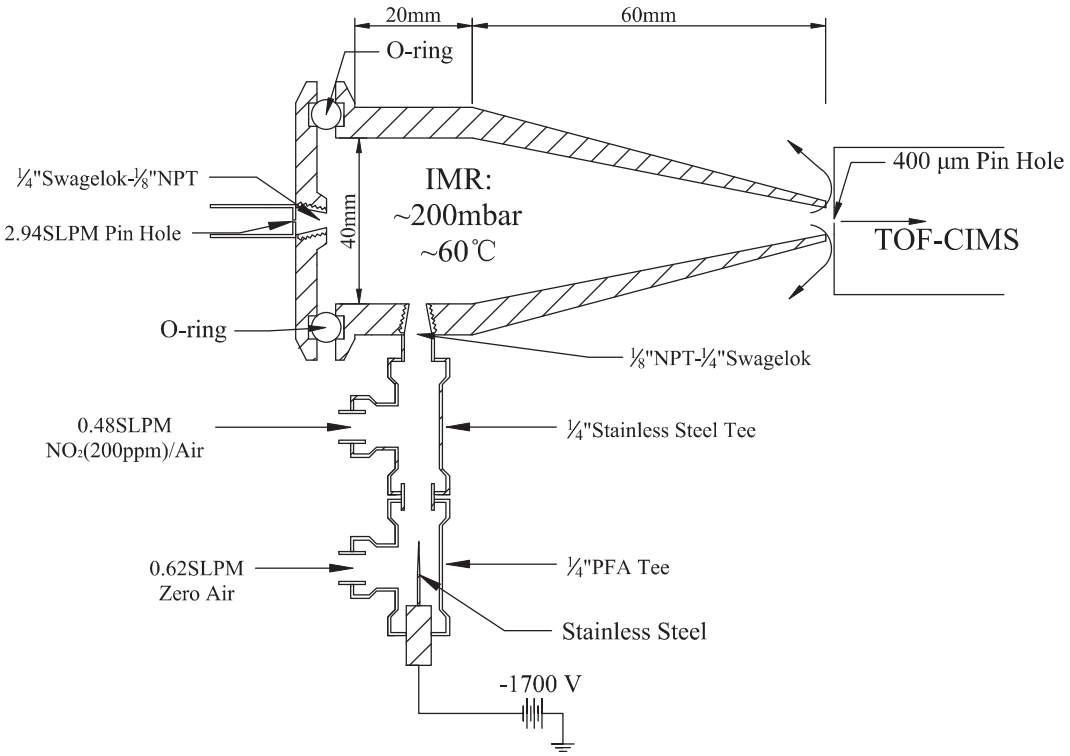

Fig. 1. Schematic diagram of the corona discharge ion source and the IMR chamber.

Gases, >99.99%) was added to act as a scavenger of OH radicals and other less stable primary ions (Nagato et al., 2006). The CD ion source was attached to the IMR chamber through a 3.2-mm tube OD stainless steel pipefitting. The IMR chamber was the original part from the manufacturer. A custom-made Teflon pinhole was installed at the front of the IMR to control the sampling flow rate at 2.94 SLPM. The typical operation pressure of the IMR was about ~200 mbar, which corresponded to an ion-molecule reaction time of ~0.14 s.

At the initial stage of negative corona discharging in air, the primary ions should be dominated by O^- and O_2^- (R5 and R6), which will react with O_2, CO_2, and H_2O to form O_3^- (R14), CO_3^- (R15) and OH^- (R12) ions within a few milliseconds (Nagato et al., 2006).

$$O^- + O_2 + M \rightarrow O_3^- \quad \text{(R14)}$$

$$O^- + CO_2 \rightarrow CO_3^- \quad \text{(R15)}$$

Although NO_x was also produced by the discharge (R9 to R11), excessive NO_2 (0.38 SLPM ~200 ppmv) were added into the downstream of the CD tube to completely convert other primary ions into more stable NO_3^- ions (R16 to R19).

$$O_2^- + NO_2 \rightarrow NO_2^- + O_2 \quad \text{(R16)}$$

$$NO_2^- + O_3 \rightarrow NO_3^- + O_2 \quad \text{(R17)}$$

$$O_3^- + NO_2 \rightarrow NO_3^- + O_2 \quad \text{(R18)}$$

$$CO_3^- + NO_2 \rightarrow NO_3^- + CO_2 \quad \text{(R19)}$$

More importantly, NO_2 can serve as OH scavenger (R13) to prevent SO_2 oxidation in the IMR region.

Fig. 2 is a typical mass spectrum obtained during a laboratory calibration. The reagent ion NO_3^- (m/z 61.988) was the dominant ion, accounting for more than 95% of the total ion signal intensity. $NO_3^-\cdot HNO_3$ (m/z 124.984) and NO_2^- (m/z 45.993) were the second and third most abundant ions but their intensities were respectively less than 4% and 1% of the intensity of NO_3^-. H_2SO_4 was detected by signal at m/z 96.960. Trace amounts of O^- (m/z 15.995), O_2^- (m/z 31.990), O_3^- (m/z 47.985), OH^- (m/z 17.003), $OH\cdot H_2O^-$ (m/z 35.014), HCO_3^- (m/z 60.993), and $HCO_3\bullet H_2O^-$ (m/z 79.004) were also detected in the spectrum, which is consistent with the proposed NO_3^- production mechanism (Nagato et al., 2006; Viggiano et al., 1997). Due to the excess NO_2, $HCO_3\cdot(H_2O)_2^-$ (m/z 97.014) and $O^-\cdot H_2O\cdot HNO_3$ (m/z 97.002) were barely detected and hence will not interfere with the sulfuric acid signal at m/z 96.960.

2.2. Gaseous H_2SO_4 calibration

Gaseous H_2SO_4 calibrations were performed using in-situ generated H_2SO_4 standards, which were quantitatively converted from OH radicals generated by photolysis of water vapor (R20) at the presence of excess SO_2 (R1 to R3).

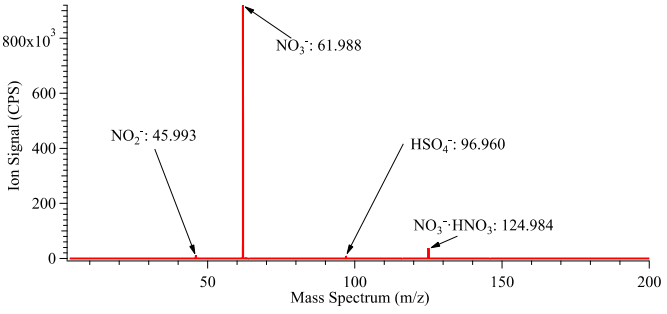

Fig. 2. A typical mass spectrum obtained in a calibration.

$H_2O + h\nu\ (\lambda = 184.9\ nm) \rightarrow OH + H$ (R20)

In principle, the calibration device was similar to that used in previous works (Berresheim et al., 2000; Kurten et al., 2012; Tanner and Eisele, 1995; Zheng et al., 2010) and the detailed description was provided in the supplementary section (see Fig. S1). The intensity of the 184.9 nm emissions from the Hg lamp was both monitored by an R5764 phototube and precisely measured with nitrous oxide (N_2O) actinometry (Edwards et al., 2003). The detailed operation procedure was provided in the supplementary section.

Fig. 3a is the time series of a typical calibration experiment. At the beginning, 4.4 SLPM (Thermo Scientific, Model 111) dry air was supplied into the inlet and the RH was decreased to 11.9%. At 48 s, 90 SCCM (Thermo Scientific 146i Dynamic Gas Calibrator) SO_2 (Nanjing Special Gases Inc., >99.9%) was injected into the sample inlet (18 cm from the CIMS inlet) and the final SO_2 mixing ratio was about 5.6 ppmv. The background signal increased by ~46 CPS, corresponding to 0.8 CPS per 100 ppbv SO_2. The reasons that can cause this SO_2 background signals are either that the molecular mean free path becomes much longer under vacuum conditions, and thus some SO_2 molecules may diffuse from IMR into the CD tube or that the CD may emit some UV light, which may produce trace amounts of OH in the IMR. Evidently, ambient level of SO_2 (typically on the order of 10 ppbv) will not cause significantly interference with H_2SO_4 measurement. The UV lamp was turned on at around 100 s. H_2SO_4 signal immediately started increasing as the lamp was warming up. By decreasing the dry air flow rate, more relatively humid room air was pulled into the inlet and the RH was accordingly increased step by step (upper panel of Fig. 3a) until reach ambient level of 27.1%. During the calibration, air temperature inside the inlet was about 23.0 ± 0.2 °C and the UV intensity was maintained steady as indicated by the phototube current measurement (2.4 ± 0.2 nA). About 30 SCCM propane (C_3H_8) (Nanjing Special Gases Inc., >99.99%) was injected into the sample inlet (~5 cm to the left of the UV window) as an OH scavenger throughout the calibration to prevent the potential interference from HO_x cycling due to reaction R21 and R22.

$H + O_2 \rightarrow HO_2$ (R21)

$HO_2 + NO \rightarrow NO_2 + OH$ (R22)

To demonstrate that ~3000 ppmv C_3H_8 was sufficient to prevent HO_2 from regenerating OH, at ~980 s C_3H_8 was switched to the front injector (indicated by the vertical dark arrow in Fig. S1) before the

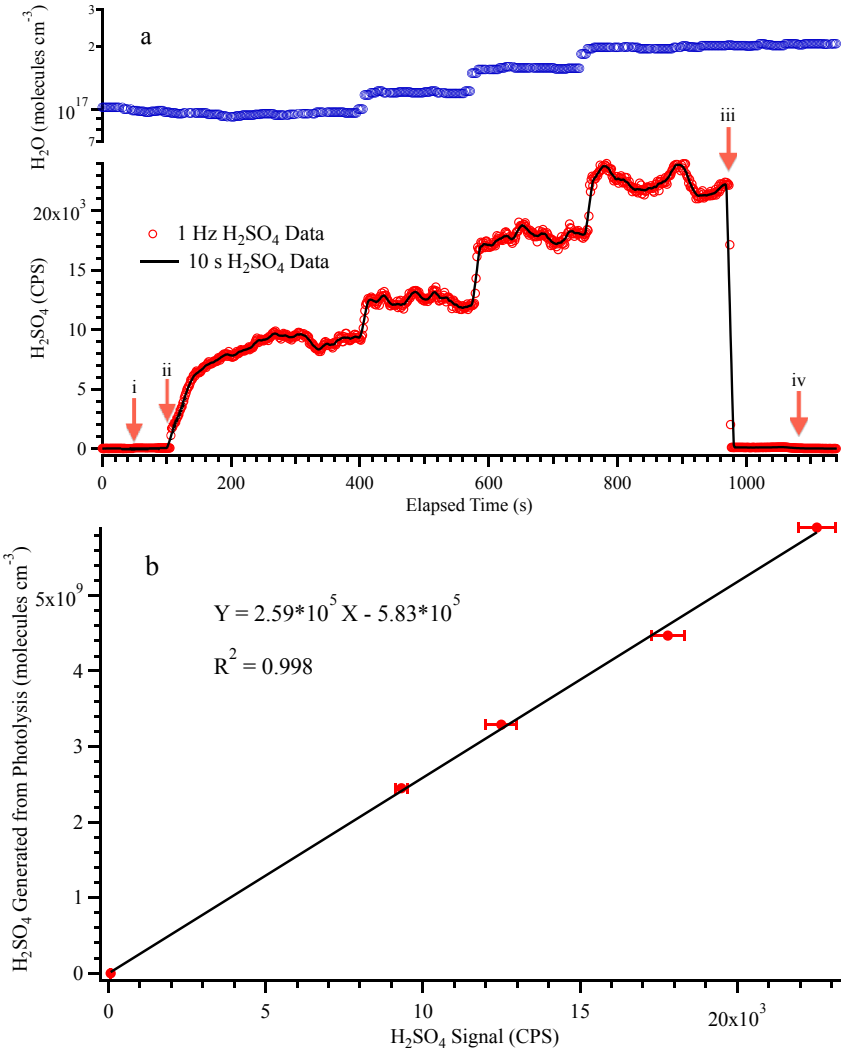

Fig. 3. a) Time series of a typical H_2SO_4 calibration experiment. Arrows i, ii, iii, and iv respectively indicate the time points when SO_2 was injected into the calibration tube, Hg lamp was turned on, C_3H_8 was injected at the front end of the sample inlet, and both Hg lamp and SO_2 flow were turned off. b) The calibration curve retrieved from the above time series.

SO_2 injection port. HSO_4^- signal immediately dropped to the same level as the background level when UV was off, indicating that all OH radicals generated from the photolysis were completely scavenged by C_3H_8. Both UV light and SO_2 injection were turned off at about 1080 s and the signal returned to the initial background level. The H_2SO_4 standards concentrations at each level of humidity were calculated according to the actinometry measurement (see supplementary section). It is worth noting that in order to maintain laminar flow inside the inlet and to increase NO_x production during the N_2O actinometry measurement, relatively low flow rate (Hanson and Eisele, 2000) and small ID inlet (see Fig. S1) were used in H_2SO_4 calibration, which led to the relatively high H_2SO_4 concentration (2.5×10^9–5.9×10^9 molecules cm^{-3}). In the future work, a CIMS based NO_x measurement technique will be used to achieve pptv-level of NO_x detection, which makes it possible to utilize bigger ID sample inlet and faster sample flow rate.

Fig. 3b is the calibration curve derived from the above calibration time series. The sensitivity of the CD-HRToF-CIMS was evaluated to be 2.59×10^5 molecules cm^{-3} per CPS normalized HSO_4^- signal.

2.3. Aerosol sulfate calibration

The CD-HRToF-CIMS can also be used to detect aerosol sulfate by incorporating with a filter inlet for gas and aerosol measurements (FIGAERO). The detailed description of FIGAERO has been given by Lopez-Hilfiker et al. (2014). Briefly, it has two independent inlet ports for simultaneous aerosol collection and gas-phase sampling. Aerosol samples are collected onto a 0.5 μm pore size 24 mm PTFE filter (PALL Corporation), which is mounted on a movable tray. After collection, the filter is automatically switched to a thermo desorption port (the middle pinhole as shown in Fig. S2), where 2.5 SLPM heated pure N_2 is blown onto the filter to thermally desorb aerosol samples into the gas phase for analysis. The sample collection time and the temperature of the N_2 carrier gas can be programmed with the Eyeon control software (Aerodyne Research Inc.). The filter collection efficiency for $PM_{2.5}$ is more than 99% (Lopez-Hilfiker et al., 2014). The performance of the FIGAERO with CD-HRToF-CIMS has been tested by laboratory generated aerosol samples and the detailed operation procedure is provided in the supplementary section.

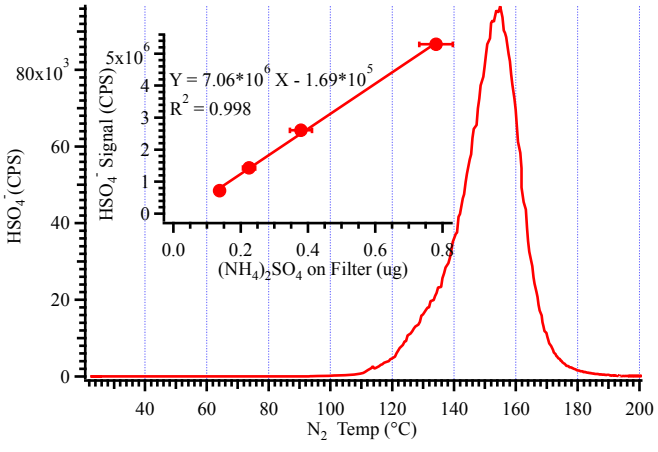

Fig. 4. A thermogram obtained from FIGAERO/CD-HRToF-CIMS calibrations. The insert is a calibration curve with different filter collection time, i.e., different aerosol sample mass. The error bars of the HSO_4^- signal are estimated from the product of the standard deviation of the thermogram baseline and the time period covered by the peak area with a value of ~1400 CPS, which is less than 0.2% of the lowest HSO_4^- signal value. The error bars of the $(NH_4)_2SO_4$ sample masses are evaluated from the standard deviation of the SMPS scans within the sample collection time.

Fig. 4 displays the thermogram of one cycle of ammonium sulfate calibration. The desorption temperature was set to increase from 25 °C up to 200 °C over 10 min and then maintained at 200 °C for another 5 min for complete desorption. HSO_4^- signal became detectable when temperature reached ~92 °C and reached peak a value at about 155 °C. The decomposition temperature of $(NH_4)_2SO_4$ (T_s) was regarded as the temperature at which the HSO_4^- signal was increasing at the highest rate. Using sigmoidal function to fit the rising portion of the thermogram, we obtained a value of 150 °C for T_s, which agreed fairly well with literature values (Qiu and Zhang, 2012). By varying collection times from 2 min to 16 min with a constant sampling flow rate of 0.64 SLPM, the mass of $(NH_4)_2SO_4$ collected on the filter ranged from about 0.14 μg to 0.81 μg. Both HSO_4^- peak height and peak area showed linear correlation with the sulfate mass concentration and peak areas were used in this work to obtain the calibration curve (insert of Fig. 4). The mass detection limit for $(NH_4)_2SO_4$ was less than 4 ng (on the filter) based on two times of the baseline noise. Given 10-min collection time and 1 SLPM collection flow rate, the corresponding ambient level of $(NH_4)_2SO_4$ was less than 0.5 μg m^{-3}. Moreover, the linear correlation coefficient of 0.998 indicated excellent collection and desorption performance of the FIGAERO/CD-HRToF-CIMS system.

3. Results and discussion

Theoretically, the sensitivity of the CD-HRToF-CIMS in H_2SO_4 measurements can be quantified according to ion–molecule reaction R4 (when n = 0) as

$$[H_2SO_4] = \alpha[HSO_4^-]/((k_4 \cdot \Delta t[NO_3^-]), \quad \text{(E1)}$$

where k_4 is the ion-molecule reaction rate coefficient of the reaction R4, Δt is the ion-molecule reaction time inside the IMR, $[HSO_4^-]$ and $[NO_3^-]$ are the ion signal intensities (denoted by counts per second, CPS) directly measured by the CD-HRToF-CIMS. To account for the variations of reagent ion signal, in this work all processed HSO_4^- signals were normalized against one million CPS NO_3^- (Zheng et al., 2008, 2011, 2013, 2015), which was the typical reagent ion intensity. The factor α in E1 is a calibration factor and its value should be 1 if the ion–molecule reaction is well defined, i.e., k_4, Δt, ion detection efficiency, and wall losses were precisely known, which was often not the case (Zheng et al., 2011). The collision-limited value of k_4 (1.89×10^{-9} cm^3 $molecule^{-1}$ s^{-1}) (Zheng et al., 2008) was used here. The reaction time, Δt, was estimated to be ~0.14 s based on plug-flow assumption. Ideally ($\alpha = 1$), one CPS HSO_4^- signal corresponded to 2.6×10^4 molecules cm^{-3} H_2SO_4 under ambient conditions, which differed from the value of 2.59×10^5 molecules cm^{-3} (determined by H_2SO_4 calibration) by a factor of 10, i.e., $\alpha = 10$ in eq. (E1). This large calibration factor was significantly different from that in our previous work (Zheng et al., 2010). The likely cause was that the IMR pressure was measured by a thermocouple type vacuum gauge, which was usually not used as a high-precision pressure transducer.

The uncertainties of CD-HRToF-CIMS measurements mostly originated from calibration procedures, flow controls, pressure and RH measurements. Due to the strong absorption of 184.9 nm emission by O_2, it was difficult to accurately map the spacial distribution of 184.9 nm emission intensities inside the inlet. Therefore, one of the most critical procedures of the H_2SO_4 calibration was to determine the actinic flux of the Hg lamp and the irradiation time or the product of $I_{184.9} \cdot t$ in eq. SE1 (Edwards et al., 2003). In this work, $I_{184.9} \cdot t$ was determined by N_2O actinometry. The advantage of the N_2O actinometry method was that N_2O was

photolyzed under the same conditions as H_2SO_4 calibrations were conducted so that all the geometric factors of the inlet were taken into account. However, the NO_x generated from N_2O photolysis was analyzed by a commercial NH_3-NO_x analyzer (Thermo Scientific, Model 17i) (NH_3 converter was bypassed in this work), the detection limit of which was about 0.5 ppbv NO_x. Evidently, higher N_2O concentration can lead to higher NO_x production and thus more accurate N_2O actinometry measurement. However, higher N_2O concentration can cause substantial change in O_2 mixing ratio and thus alter the 184.9 nm emission intensities within the inlet. Consequently, 6.5% of N_2O was used in this work and the uncertainty associated with the $I_{184.9} \cdot t$ measurement was about 25%, mainly propagated from the NO_x detection. The RH sensor was estimated to contribute ~3% to the measurement uncertainty. All flow controls were achieved with critical orifices and Swagelok stainless steel needle valves, which were all calibrated with a Gilibrator with a measurement uncertainty of <1% each. We found the pressure reading was reproducible within 2% of averaged value during calibrations. Therefore the overall measurement uncertainty of the CD-HRToF-CIMS was about 34%.

The detection limit (DL) was found to be 3.1×10^5 molecules cm^{-3} for 10-s average time and two times of the baseline noise. This DL was several times higher than our previous work using API-ID-CIMS (Zheng et al., 2010) and that was mainly due to the much lower IMR pressure in this work that caused significant expansion dilution of the H_2SO_4 sample. However, the sensitivity of the CD-HRToF-CIMS was still reasonably high enough for the measurement of ambient level of H_2SO_4, which was typically on the order of 10^6 molecules cm^{-3} or higher (Zheng et al., 2011).

4. Conclusion

A new corona discharge (CD) based ion source was successfully developed for the HRToF-CIMS to conduct both gas-phase sulfuric acid and aerosol-phase sulfate measurements (by incorporating with a FIGAERO interface). The detection principle was based on the well-established NO_3^- ion chemistry. The unique character of the CD ion source was such that NO_3^- was generated in a two-step scheme using pure air and NO_2 (200 ppmv) as the reagent gases. Primary ions and OH radicals generated in the CD can be converted into more stable NO_3^- ions and HNO_3 by reaction with excess NO_2. The CD-HRToF-CIMS showed no detectable interference from hundreds ppbv of SO_2, well above the typical ambient level. Since neither radioactive material nor highly corrosive chemicals were used, the CD-HRToF-CIMS can be readily field deployed. The CD ion source had the advantages of low cost and a simple but robust structure. Unlike the atmospheric pressure ionization scheme, the CD ion source was integrated onto the IMR chamber, which made it possible to measure aerosol sulfate by coupling to a FIGAERO interface. Moreover, unlike a quadrupole-based mass spectrometer, the desired HSO_4^- signal was detected by its exact mass of m/z 96.960, which was well resolved from the potential interferences of $HCO_3^- \cdot (H_2O)_2$ (m/z 97.014) and $O^- \cdot H_2O \cdot HNO_3$ (m/z 97.002). In this work, using laboratory-generated standards the CD-HRToF-CIMS was demonstrated to be able to detect as low as 3.1×10^5 molecules cm^{-3} gaseous H_2SO_4 and 0.5 μg m^{-3} ammonium sulfate based on 10-s integration time and 2σ of the baseline noise. Although the sensitivity of the CD-HRToF-CIMS was significantly less than that of an API-NO_3^--CIMS in term of H_2SO_4 detection, its detection limit was substantially lower than the threshold H_2SO_4 concentration during nucleation events (Kulmala et al., 2013, 2014; Zheng et al., 2011). The CD ion source can highly expand the capability of the HRToF-CIMS in both field measurements and laboratory studies, including chamber simulations and flow tube experiments (Young et al., 2008). The CD-HRToF-CIMS was demonstrated to be a promising tool for studies of aerosol formation mechanism and the chemical processes that are critical to understand the evolution of aerosols in the atmosphere.

Acknowledgments

This work is supported by the National Natural Science Foundation of China (41275142, 41575122, and 21377059), Jiangsu Natural Science Foundation (BK2012861), Jiangsu Provincial Specially-Appointed Professors Foundation, and International Science & Technology Collaborative Project of China (2014DFA90780). The authors are grateful to Dr. Douglas R. Worsnop, Dr. John. B. Nowak and Dr. Joel R. Kimmel from Aerodyne for their support on the HRToF-CIMS instrumentation.

Appendix A. Supplementary data

Supplementary data related to this article can be found at http://dx.doi.org/10.1016/j.atmosenv.2015.08.028.

References

Andrade, F.J., Shelley, J.T., Wetzel, W.C., Webb, M.R., Gamez, G., Ray, S.J., Hieftje, G.M., 2008. Atmospheric pressure chemical ionization source. 1. Ionization of compounds in the gas phase. Anal. Chem. 80, 2646–2653.

Berresheim, H., Elste, T., Plass-Dulmer, C., Eisele, F.L., Tanner, D.J., 2000. Chemical ionization mass spectrometer for long-term measurements of atmospheric OH and H_2SO_4. Int. J. Mass Spectrom. 202, 91–109.

Edwards, G.D., Cantrell, C.A., Stephens, S., Hill, B., Goyea, O., Shetter, R.E., Mauldin, R.L., Kosciuch, E., Tanner, D.J., Eisele, F.L., 2003. Chemical ionization mass spectrometer instrument for the measurement of tropospheric HO_2 and RO_2. Anal. Chem. 75, 5317–5327.

Eisele, F.L., Tanner, D.J., 1993. Measurement of the gas-phase concentration of H_2so_4 and methane sulfonic-acid and estimates of H_2so_4 production and loss in the atmosphere. J. Geophys. Res. 98, 9001–9010.

Finlayson-Pitts, B.J., Pitts, J.N., 1999. Chemistry of the Upper and Lower Atmosphere : Theory, Experiments and Applications. Academic Press, San Diego, Calif.

Franzblau, E., 1991. Electrical discharges involving the formation of NO, NO_2, HNO_3, and O_3. J. Geophys. Res. Atmos. 96, 22337–22345.

Hanson, D.R., Eisele, F., 2000. Diffusion of H_2SO_4 in humidified nitrogen: hydrated H_2SO_4. J. Phys. Chem. A 104, 1715–1719.

Huey, L.G., 2007. Measurement of trace atmospheric species by chemical ionization mass spectrometry: speciation of reactive nitrogen and future directions. Mass Spectrom. Rev. 26, 166–184.

IPCC, 2007. IPCC Fourth Assessment Report: Climate Change 2007: The Physical Science Basis. Cambridge Univ. Press, United Kingdom and New York.

Jimenez, J.L., Canagaratna, M.R., Donahue, N.M., Prevot, A.S.H., Zhang, Q., Kroll, J.H., DeCarlo, P.F., Allan, J.D., Coe, H., Ng, N.L., Aiken, A.C., Docherty, K.S., Ulbrich, I.M., Grieshop, A.P., Robinson, A.L., Duplissy, J., Smith, J.D., Wilson, K.R., Lanz, V.A., Hueglin, C., Sun, Y.L., Tian, J., Laaksonen, A., Raatikainen, T., Rautiainen, J., Vaattovaara, P., Ehn, M., Kulmala, M., Tomlinson, J.M., Collins, D.R., Cubison, M.J., Dunlea, E.J., Huffman, J.A., Onasch, T.B., Alfarra, M.R., Williams, P.I., Bower, K., Kondo, Y., Schneider, J., Drewnick, F., Borrmann, S., Weimer, S., Demerjian, K., Salcedo, D., Cottrell, L., Griffin, R., Takami, A., Miyoshi, T., Hatakeyama, S., Shimono, A., Sun, J.Y., Zhang, Y.M., Dzepina, K., Kimmel, J.R., Sueper, D., Jayne, J.T., Herndon, S.C., Trimborn, A.M., Williams, L.R., Wood, E.C., Middlebrook, A.M., Kolb, C.E., Baltensperger, U., Worsnop, D.R., 2009. Evolution of organic aerosols in the atmosphere. Science 326, 1525–1529.

Kukui, A., Ancellet, G., Le Bras, G., 2008. Chemical ionisation mass spectrometer for measurements of OH and peroxy radical concentrations in moderately polluted atmospheres. J. Atmos. Chem. 61, 133–154.

Kulmala, M., Kontkanen, J., Junninen, H., Lehtipalo, K., Manninen, H.E., Nieminen, T., Petaja, T., Sipila, M., Schobesberger, S., Rantala, P., Franchin, A., Jokinen, T., Jarvinen, E., Aijala, M., Kangasluoma, J., Hakala, J., Aalto, P.P., Paasonen, P., Mikkila, J., Vanhanen, J., Aalto, J., Hakola, H., Makkonen, U., Ruuskanen, T., Mauldin, R.L., Duplissy, J., Vehkamaki, H., Back, J., Kortelainen, A., Riipinen, I., Kurten, T., Johnston, M.V., Smith, J.N., Ehn, M., Mentel, T.F., Lehtinen, K.E.J., Laaksonen, A., Kerminen, V.M., Worsnop, D.R., 2013. Direct observations of atmospheric aerosol nucleation. Science 339, 943–946.

Kulmala, M., Petaja, T., Ehn, M., Thornton, J., Sipila, M., Worsnop, D.R., Kerminen, V.M., 2014. Chemistry of atmospheric nucleation: on the recent advances on precursor characterization and atmospheric cluster composition in connection with atmospheric new particle formation. Annu. Rev. Phys. Chem. 65, 21–37, 65.

Kurten, A., Rondo, L., Ehrhart, S., Curtius, J., 2011. Performance of a corona ion source for measurement of sulfuric acid by chemical ionization mass spectrometry. Atmos. Meas. Tech. 4, 437–443.

Kurten, A., Rondo, L., Ehrhart, S., Curtius, J., 2012. Calibration of a chemical

ionization mass spectrometer for the measurement of gaseous sulfuric acid. J. Phys. Chem. A 116, 6375–6386.
Lopez-Hilfiker, F.D., Mohr, C., Ehn, M., Rubach, F., Kleist, E., Wildt, J., Mentel, T.F., Lutz, A., Hallquist, M., Worsnop, D., Thornton, J.A., 2014. A novel method for online analysis of gas and particle composition: description and evaluation of a filter inlet for gases and AEROsols (FIGAERO). Atmos. Meas. Tech. 7, 983–1001.
Mauldin, R.L., Cantrell, C.A., Zondlo, M., Kosciuch, E., Eisele, F.L., Chen, G., Davis, D., Weber, R., Crawford, J., Blake, D., Bandy, A., Thornton, D., 2003. Highlights of OH, H_2SO_4, and methane sulfonic acid measurements made aboard the NASA P-3B during transport and chemical evolution over the Pacific. J. Geophys. Res. 108.
Mauldin, R.L., Berndt, T., Sipila, M., Paasonen, P., Petaja, T., Kim, S., Kurten, T., Stratmann, F., Kerminen, V.M., Kulmala, M., 2012. A new atmospherically relevant oxidant of sulphur dioxide. Nature 488, 193–196.
Nagato, K., Matsui, Y., Miyata, T., Yamauchi, T., 2006. An analysis of the evolution of negative ions produced by a corona ionizer in air. Int. J. Mass Spectrom. 248, 142–147.
Qiu, C., Zhang, R.Y., 2012. Physiochemical properties of alkylaminium sulfates: hygroscopicity, thermostability, and density. Environ. Sci. Technol. 46, 4474–4480.
Seinfeld, J.H., Pandis, S.N., 1998. Atmospheric Chemistry and Physics: from Air Pollution to Climate Change. Wiley, New York.
Sekimoto, K., Takayama, M., 2007. Influence of needle voltage on the formation of negative core ions using atmospheric pressure corona discharge in air. Int. J. Mass Spectrom. 261, 38–44.
Sipila, M., Berndt, T., Petaja, T., Brus, D., Vanhanen, J., Stratmann, F., Patokoski, J., Mauldin, R.L., Hyvarinen, A.P., Lihavainen, H., Kulmala, M., 2010. The role of sulfuric acid in atmospheric nucleation. Science 327, 1243–1246.
Skalny, J.D., Orszagh, J., Mason, N.J., Rees, J.A., Aranda-Gonzalvo, Y., Whitmore, T.D., 2008. Mass spectrometric study of negative ions extracted from point to plane negative corona discharge in ambient air at atmospheric pressure. Int. J. Mass Spectrom. 272, 12–21.
Tanner, D.J., Eisele, F.L., 1995. Present OH measurement limits and associated uncertainties. J. Geophys. Res. 100, 2883–2892.
Tanner, D.J., Jefferson, A., Eisele, F.L., 1997. Selected ion chemical ionization mass spectrometric measurement of OH. J. Geophys. Res. 102, 6415–6425.
Viggiano, A.A., Seeley, J.V., Mundis, P.L., Williamson, J.S., Morris, R.A., 1997. Rate constants for the reactions of XO_3-(H_2O)(n) (X = C, HC, and N) and NO3-(HNO3)(n) with H2SO4: implications for atmospheric detection of H2SO4. J. Phys. Chem. A 101, 8275–8278.
Young, L.H., Benson, D.R., Kameel, F.R., Pierce, J.R., Junninen, H., Kulmala, M., Lee, S.H., 2008. Laboratory studies of H_2SO_4/H_2O binary homogeneous nucleation from the SO_2+OH reaction: evaluation of the experimental setup and preliminary results. Atmos. Chem. Phys. 8, 4997–5016.
Zhang, R.Y., 2010. Getting to the critical nucleus of aerosol formation. Science 328, 1366–1367.
Zhang, R.Y., Khalizov, A., Wang, L., Hu, M., Xu, W., 2012. Nucleation and growth of nanoparticles in the atmosphere. Chem. Rev. 112, 1957–2011.
Zheng, J., Zhang, R., Fortner, E.C., Volkamer, R.M., Molina, L., Aiken, A.C., Jimenez, J.L., Gaeggeler, K., Dommen, J., Dusanter, S., Stevens, P.S., Tie, X., 2008. Measurements of HNO_3 and N_2O_5 using ion drift-chemical ionization mass spectrometry during the MILAGRO/MCMA-2006 campaign. Atmos. Chem. Phys. 8, 6823–6838.
Zheng, J., Khalizov, A., Wang, L., Zhang, R., 2010. Atmospheric pressure-ion drift chemical ionization mass spectrometry for detection of trace gas species. Anal. Chem. 82, 7302–7308.
Zheng, J., Hu, M., Zhang, R., Yue, D., Wang, Z., Guo, S., Li, X., Bohn, B., Shao, M., He, L., Huang, X., Wiedensohler, A., Zhu, T., 2011. Measurements of gaseous H_2SO_4 by AP-ID-CIMS during care Beijing 2008 Campaign. Atmos. Chem. Phys. 11, 7755–7765.
Zheng, J., Garzón, J.P., Huertas, M.E., Zhang, R., Levy, M., Ma, Y., Huertas, J.I., Jardón, R.T., Ruíz, L.G., Tan, H., Molina, L.T., 2013. Volatile organic compounds in Tijuana during the Cal-Mex 2010 campaign: measurements and source apportionment. Atmos. Environ. 70, 521–531.
Zheng, J., Ma, Y., Chen, M., Zhang, Q., Wang, L., Khalizov, A.F., Yao, L., Wang, Z., Wang, X., Chen, L., 2015. Measurement of atmospheric amines and ammonia using the high resolution time-of-flight chemical ionization mass spectrometry. Atmos. Environ. 102, 249–259.